SUPPLEMENTAL MATERIAL

Assessment of image quality

The image quality of late gadolinium-enhanced MRI datasets was graded by 2 observers in consensus, according to the following 4 point scale: 0 – severe motion artifacts or inversion time inaccuracy, 1 – moderate motion artifacts or inversion time inaccuracy, 2 – mild motion artifacts or inversion time inaccuracy, 3 – no motion artifacts or inversion time inaccuracy. Only the datasets with image quality score 2 or 3, corresponding to good or excellent image quality, were considered eligible for global fibrosis quantification. Only the datasets with image quality 3, corresponding to excellent image quality, were considered eligible for regional fibrosis characterization. Image quality was graded 0 in 1 patient, 1 in 3 patients, 2 in 17 patients, and 3 in 20 patients. Therefore, 37/41 patients were eligible for global fibrosis quantification, and 20/41 for regional fibrosis characterization.

Reproducibility of atrial fibrosis quantification

The segmentation of atrial fibrosis was performed by using the method described by Oakes et al. (1). According to this method, the optimal threshold is set by analyzing the histogram of voxels from the left atrial wall. In this study, the same threshold was also applied on the right atrium in order to quantify biatrial fibrosis. Because the threshold did not differ between the left and right atrium, reproducibility was only analyzed for left atrium fibrosis quantification. Intra- and inter-observer agreement for the quantification of left atrial fibrosis were assessed by using intra-class correlation coefficients and Bland and Altman analyses, based on the segmentation of 20 datasets from 2 independent observers blinded from clinical characteristics. Intra-observer agreement for the quantification of left atrial fibrosis was good (ICC=0.95, $P<0.0001$, mean bias 0.2%, 95% limits of agreement from -4.0 to +4.4%). Inter-observer

agreement was also good (ICC=0.93, P<0.0001, mean bias 0.4%, 95% limits of agreement from -5.2 to +5.8%).

Computation of Local Fibrosis Descriptors

Atrial meshes from late gadolinium-enhanced MRI scans were built using a previously described image-processing pipeline (2-4). From the segmented images, a shape-based interpolation technique (5) was applied to generate a high-resolution image stack with an isotropic voxel size of 400 μm^3. A finite element tetrahedral mesh was generated from this image stack using an octree-based meshing technique described previously (6), which generated boundary-fitted, locally refined, and smooth surfaces. The resulting meshes had 1 to 2.2 million nodes and 5.4 to 11.3 million elements, with average edge length of 400 μm. Each element was labeled as fibrotic or non-fibrotic based on the intensity of the corresponding voxel in the high-resolution image stack. For each atrial mesh, a map of local fibrosis density (LFD) was constructed. At each node, surrounding tissue elements within a volume of 5 mm radius were identified using a KD-tree (7). Then, the LFD value for that node was calculated based on corresponding values of these parameters for all elements within each local volume. LFD values indicated the proportion of fibrotic elements by volume (i.e., the number of fibrotic elements divided by the total number of elements).

Definition of reentrant activity threshold

In order to compare local fibrosis characteristics between regions with high and low levels of reentrant activity, a threshold was defined on absolute values of reentry statistics. On each point of the geometry, this refers to the probability of observing a reentry at a given time frame. To set the threshold value, we have analyzed its impact on the size of reentrant regions (expressed as % of the surface). This relationship is illustrated in Supplemental Figure 3. The rationale is that the only validation available to

define such a threshold is the result from ablation. Indeed, this threshold has to be consistent with the area usually ablated before reaching ablation endpoints. A too high threshold would not be clinically relevant, as it would only describe a very little atrial surface. Conversely, a too low threshold defining most of the atrium as a reentrant driver would not be relevant either as it would not match what we observe when performing ablation in patients. Unfortunately, the area covered by ablation on each driver region before reaching local ablation endpoints was not available in the studied population as 3D electroanatomical mapping systems were not routinely used. Therefore, a rotor likelihood threshold of 0.002 was chosen, as the regions defined as drivers when applying this threshold covered 10 to 15% of the atrial surface.

SUPPLEMENTAL REFERENCES

1. Oakes RS, Badger TJ, Kholmovski EG, et al. Detection and Quantification of Left Atrial Structural Remodeling Using Delayed Enhancement MRI in Patients with Atrial Fibrillation. Circulation. 2009 Apr 7;119(13):1758–67.
2. Vadakkumpadan F, Rantner LJ, Tice B, Boyle P, Prassl AJ, Vigmond E, et al. Image-based models of cardiac structure with applications in arrhythmia and defibrillation studies. Journal of electrocardiology. 2009;42(2):157 e1-10.
3. McDowell KS, Vadakkumpadan F, Blake R, Blauer J, Plank G, MacLeod RS, et al. Methodology for patient-specific modeling of atrial fibrosis as a substrate for atrial fibrillation. Journal of electrocardiology. 2012;45(6):640-5.
4. McDowell KS, Vadakkumpadan F, Blake R, Blauer J, Plank G, Macleod RS, et al. Mechanistic inquiry into the role of tissue remodeling in fibrotic lesions in human atrial fibrillation. Biophysical journal. 2013;104(12):2764-73.
5. Raya SP, Udupa JK. Shape-based interpolation of multidimensional objects. IEEE transactions on medical imaging. 1990;9(1):32-42.

6. Prassl AJ, Kickinger F, Ahammer H, Grau V, Schneider JE, Hofer E, et al. Automatically generated, anatomically accurate meshes for cardiac electrophysiology problems. IEEE transactions on bio-medical engineering. 2009;56(5):1318-30.
7. Rusu RB, Cousins S, editors. 3D is here: Point Cloud Library (PCL). Robotics and Automation (ICRA), 2011 IEEE International Conference on; 2011 9-13 May 2011.

SUPPLEMENTAL FIGURES

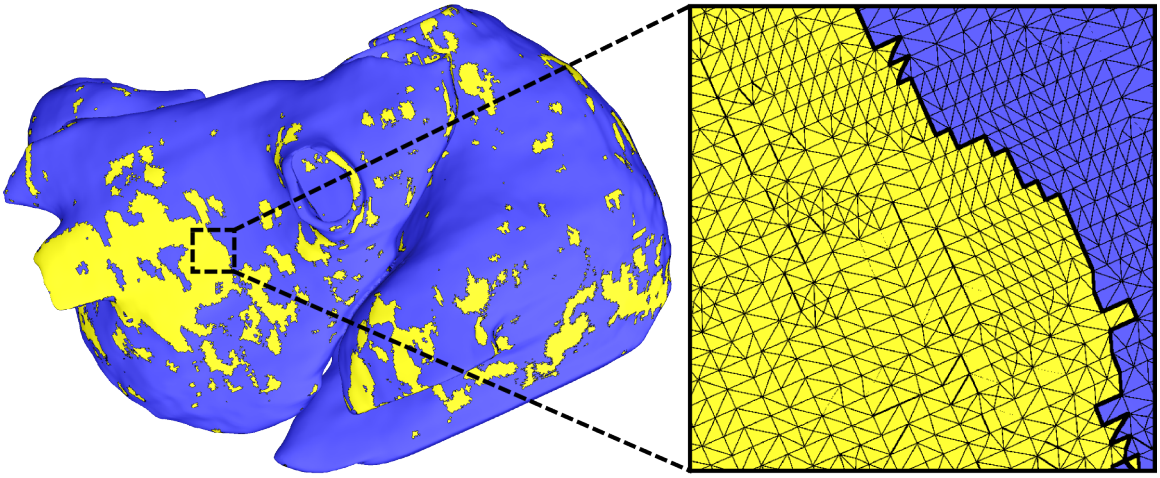

Supplemental Figure 1: A finite-element tetrahedral mesh of the atria was automatically generated from MRI using an octree meshing technique that creates boundary-fitted, locally-refined and smooth surfaces.

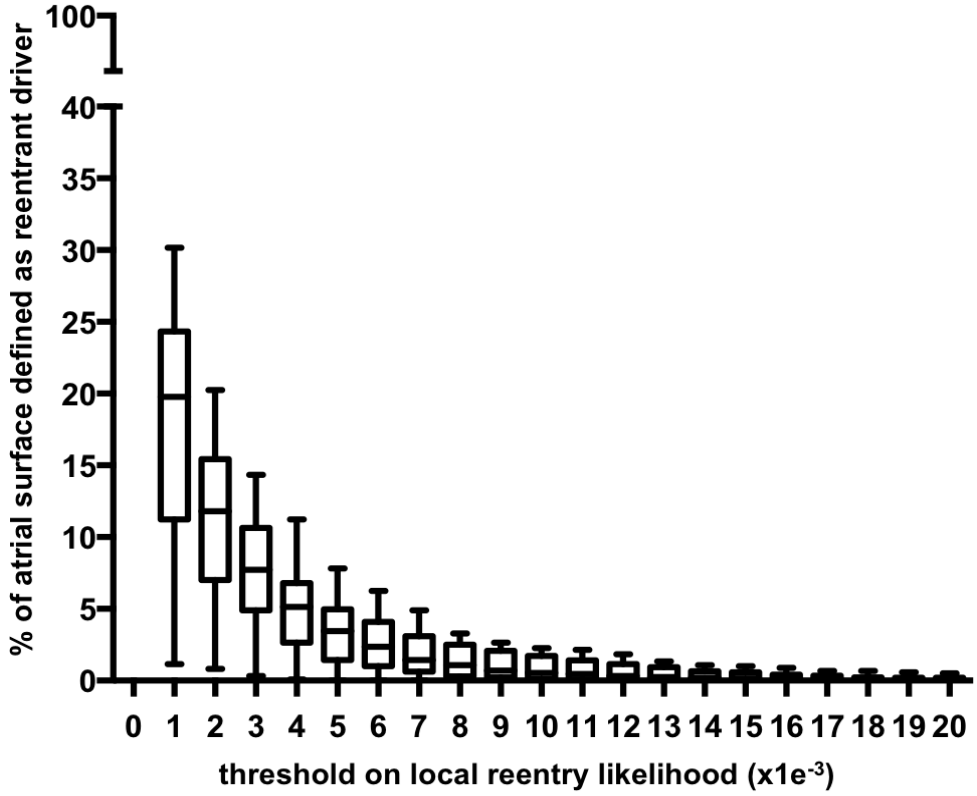

Supplemental Figure 2: Relationship between the threshold applied on reentry statistics and the area defined as reentrant drivers when applying this threshold.